Numerical Simulation of a High Power Stirling Cryocooler

Y. C. Cai, Y. Xu, D. M. Sun, Q. Shen, Z. Z. Cheng, X. Zhao, J. Zhang

Institute of Refrigeration and Cryogenics, Zhejiang University
Hangzhou, P.R. China 310027

ABSTRACT

High-power Stirling cryocoolers driven by crank-rod mechanisms are promising candidates for high temperature superconductivity technologies, due to their high efficiency, wide temperature range, fast cool-down and compact structure. A high-power Stirling cryocooler was analyzed by a numerical simulation using the SAGE software. The analysis shows the phasors for mass flow rate and pressure for the working fluid, the distribution of PV power and enthalpy flow, and the temperature profile in the regenerator. The simulation shows that the cold head is able to reach a no-load refrigeration temperature of 38 K and a cooling power of 1012 W at 77.35 K with a PV power of 7.72 kW. Based on the theoretical analysis, three approaches to optimize the cryocooler have been proposed. The first one is to adjust the phase between the piston and the displacer to get an optimum phase difference between the flow and pressure at both ends of the regenerator. The second one is to make the refrigeration system behave as a resistance to match an AC motor. The third one is to optimize the size of the regenerator to a given working condition.

INTRODUCTION

The application of superconducting technology will lead to another revolution in human productivity. The fact that the critical temperature of superconductivity broke through liquid nitrogen temperature in 1986 makes the application of the superconducting technology possible [1]. With the on-going development of superconducting material and cryogenic technology, the high-power regenerative cryocoolers, such as the Gifford-McMahon (G-M) cryocoolers, the Stirling cryocoolers, and the pulse tube cryocooler [2, 3], are urgently required to cool down the superconducting devices instead of using liquid nitrogen [4]. Compared with the others, a high-power Stirling cryocooler driven by crank-rod mechanisms has several remarkable advantages, such as high efficiency, wide temperature range, fast cool-down, and compact structure [5, 6].

The thermodynamic cycle of a Stirling cryocooler widely utilized at present deviates from the ideal Stirling cycle composed of two isothermal and two isochoric processes. Research on the real Stirling cycle is always an important topic in the academic and engineering fields. In 1954, the first practical single-stage Stirling cryocooler driven by crank-rod mechanisms was built by Dutch Philips, and has been transformed into industrial products successfully due to a mature technology and high performance [7]. However, openly reported literature on this kind of

Cryocoolers 18, edited by S.D. Miller and R.G. Ross, Jr.

cryocooler is lacking because of its commercialization. Furthermore, The Stirling cryocooler was analyzed by the conventional methods of isothermal and adiabatic models [8], which are simplified. There will always be a large difference between simulated and experimental results in this type of analysis.

In this paper, the complete mathematical and physical model of a high-power Stirling cryocooler was built using SAGE [9], commercial simulation software for Stirling cycle engines. Based on the analysis of the simulation, the complicated fluid flow and heat transfer processes inside the cryocooler is revealed, showing several reasonable directions to optimize the performance of the high-power Stirling cryocooler.

SIMULATION OF A STIRLING CRYOCOOLER

Cryocooler Structure

Figure 1 shows the structure of a Stirling cryocooler driven by a crank-rod mechanism [10]. The integrated Stirling cryocooler consists of a motor, a set of crank-rod mechanisms, a compression piston, an aftercooler, a regenerator, a displacer, a cold heat exchanger, a compression space and an expansion space. The piston and displacer are driven by one set of crank-rod mechanisms, but the crank angles are different so that the volume phase of the expansion space leads the compression space to obtain efficient refrigeration [10].

Modeling

SAGE is 1-D numerical simulation software specialized in simulating and optimizing Stirling engines, Stirling cryocoolers and pulse tube cryocoolers. In the SAGE graphical interface, different parts of the machine are simulated separately with corresponding elements in the root level, and are connected to each other by mass flows and energy flows. One dimensional heat transfer and flow processes inside the cryocooler are calculated based on empirical correlations of cyclic flow [11]. Figure 2 shows the root level of the SAGE model of the Stirling cryocooler.

The working and structural parameters of the Stirling cryocooler are shown in Table 1 and Table 2 [12].

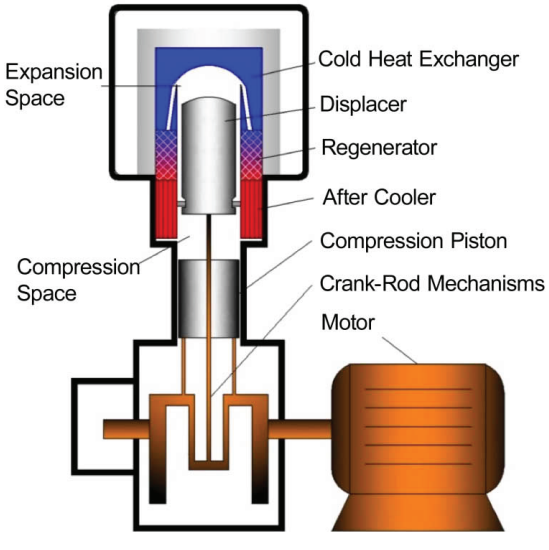

Figure 1. Schematic diagram of a Stirling cryocooler driven by crank-rod mechanisms

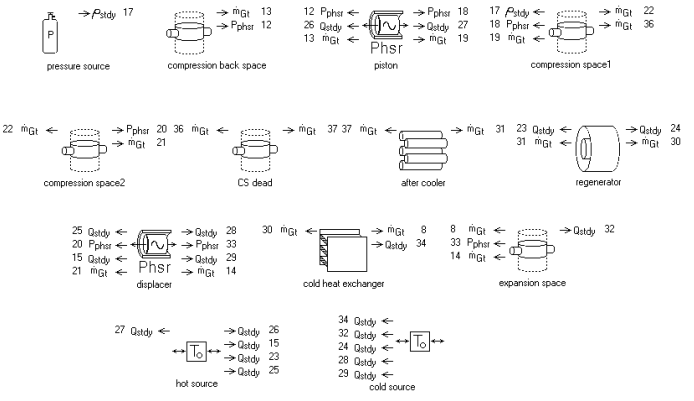

Figure 2. SAGE model of the Stirling cryocooler

Table 1. Working Parameters of the Stirling cryocooler

Working Fluid	Mean Pressure/ MPa	Refrigeration Temperature/ K	Ambient Temperature /K	Rotating Speed of Motor/ rpm
Hydrogen	2.65	77.35	300	1450

Table 2. Structural Parameters of the Stirling cryocooler

Compression Piston Stroke/ mm	Displacer Stroke /mm	Regenerator matrix	Aftercooler	Cold Heat Exchanger
52	30	Random Copper fiber	Shell-and-Tube Heat Exchanger	Slit Heat Exchanger

SIMULATION RESULTS

Phasor Diagram

The crank-rod mechanisms are driven by the motor at a constant speed of 1450 rpm drive, and the piston and displacer move sinusoidally. All the oscillating variables such as the pressure, the temperature, and the mass flow rate, are assumed to vary sinusoidally with time. Those variables are represented by a vector-like quantity called a phasor. A phasor has a length which is equal to the amplitude of the oscillation, and an angle relative to the real axis which represents its transient phase angle. The projection of these phasors on the real axis gives the instantaneous value of the variable as the phasor rotates about the axis in a counterclockwise direction with angular frequency $\omega=2\pi f$ with the constant angle difference [13].

The conservation of mass equation is represented by connecting the related phasors together to form a closed figure. The conservation of mass equation in different parts of the cryocooler is

$$\dot{m}_{in} - \dot{m}_{out} = \frac{dM}{dt} = M\left(\frac{1}{P}\frac{dP}{dt} + \frac{1}{V}\frac{dV}{dt} - \frac{1}{T}\frac{dT}{dt}\right) \tag{1}$$

where V is the gas volume; P is the dynamic pressure of gas; T is the gas temperature.

For the working space, the pressure drop and temperature variation along the space is ignored and Eq. (1) turns into Eq. 2.

$$\dot{m}_{in} - \dot{m}_{out} = \frac{\dot{P}V}{2RT} + \frac{P\dot{V}}{RT} - \frac{PV\dot{T}}{RT^2} \tag{2}$$

where $\dot{P}$, $\dot{V}$, $\dot{T}$ are the length-averaged instantaneous pressure, volume, temperature in the working space; V is the average volume; P and T are the time and length-averaged pressure and temperature of working gas.

For the heat exchanger, the temperature variation is ignored and the gas volume is constant, so Eq. (1) turns into Eq. 3.

$$\dot{m}_{in} - \dot{m}_{out} = \frac{\dot{P}V}{RT} \tag{3}$$

where $\dot{P}$ is the length-averaged instantaneous pressure in the heat exchanger; V is the volume; T is the time and length-averaged temperature of working gas.

For the regenerator that spans a large temperature difference, a log-mean averaged temperature distribution is used in the equation. The pressure drop is also ignored and the gas volume is constant, so Eq. (1) turns into Eq. 4.

$$\dot{m}_{in} - \dot{m}_{out} = \frac{\dot{P}V}{RT} - \frac{PV\dot{T}}{RT_h T_c} \tag{4}$$

where T, T_h, T_c are the log-mean averaged temperature along the regenerator, the ambient end temperature, and the cold end temperature of the regenerator, respectively.

All of the above average values of these oscillating variables can be calculated with SAGE as harmonic approximations. Figure 3 shows the phasors of mass flow rate in different parts of the cryocooler. The phasors of mass flows is closed everywhere as expected except in the regenerator, because about 50 kPa pressure drop along the regenerator is ignored to simplify the calculation. As the PV power flow is proportional to the component of the mass flow in phase with the pressure, minimizing the phase difference between the flow and pressure is necessary to get a large PV power [13]. Typically the flow at the cold end of the regenerator should lag the pressure by about 30°, meanwhile the flow leads the pressure by about 30° at the ambient end of the regenerator [14]. However, for the Stirling cryocooler in the present study, the calculation results show that the flow at the cold end of the regenerator lags the pressure by 41.6°, while at the ambient end the flow lags the pressure by 7.1°. In order to improve the performance of the cryocooler, the phase of the piston and displacer should be optimized to obtain the desired phase difference between flow and pressure at both ends of the regenerator.

Energy Flows

Figure 4 shows the distribution of time-averaged enthalpy flow and PV power [15] in the cryocooler. The dimensionless position is obtained by dividing the actual lengths of different parts by the total length of the cryocooler.

The motor inputs power, W_{CS}, into the system by driving the crank-rod mechanism to increase both the enthalpy and PV power inside the compression space. At the end of the compression space, most of the enthalpy flows into the aftercooler and decreases as the compression heat is taken away by the chill water (Q_H), while the rest flows into the seal between the cylinder and the displacer. In the real regenerator, physical properties such as specific heat vary with temperature. So, the time-averaged enthalpy inside the regenerator is not zero but about 350 W, which will degrade refrigeration performance. The PV power inside the regenerator varies along the dimensionless position because of temperature variation. In the cold heat exchanger, the enthalpy increases because the working fluid absorbs heat (Q_C) from the heat load. In the expansion space, the working fluid expands and does work W_{ES} on the displacer, and the PV power decreases.

Load Curve

According to the analysis of energy flows inside the system, the cooling power of the cryocooler equals the heat load absorbed by the cold head, and the input PV power equals to the

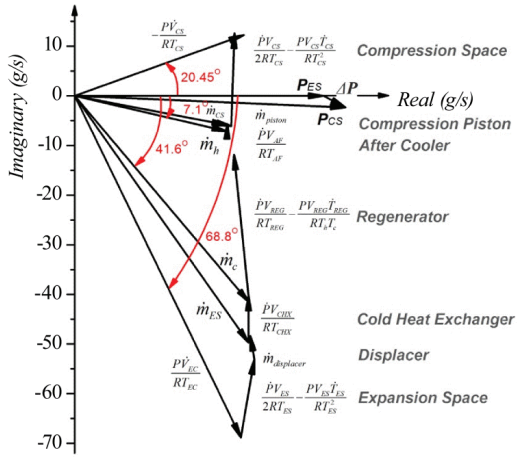

Figure 3. Phase diagram of mass flow rate of the cryocooler

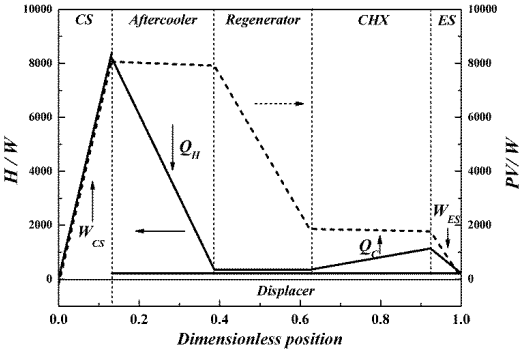

Figure 4. Distribution of energy flows in the cryocooler

power that the piston does to the working space minus the power that the working fluid does to the displacer.

Figure 5 shows the simulated load curve of the Stirling cryocooler. The cold head is able to reach the no-load refrigeration temperature of 38 K and a cooling power of 1012 W at 77.35 K with a PV power of 7.72 kW. The rated power of the motor is 11 kW, which has not been fully utilized because the friction of the crank-rod mechanisms and the reactive power consumed by the motor power. The cooler coupled to an AC motor usually behaves as a capacitance or an inductance. With such a load, the phase of the current is difference from the voltage in the AC circuit. So the available power which can be inputted into the refrigeration system is less than the rated power of the motor. The ratio of the available power and the rated power is called the power factor [16]. As the efficiency of the whole system, including the motor, increases with the power factor, optimization measures should be taken to increase the factor. Suitable capacitance and inductance need to be added to the system model to make the refrigeration system behave as a resistance to the motor, so that the motor's power factor can increase to 1, indicating a high efficiency of the system.

Temperature Profile of Regenerator

The regenerator is the key part of a cryocooler, where the cold fluid and hot fluid flow alternately from different ends, and exchange heat with the matrix periodically. Figure 6 shows the time-averaged temperature distribution of working fluid along the regenerator under

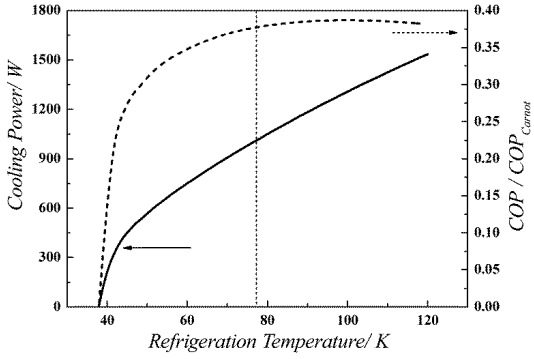

Figure 5. Simulated load curve of the stirling cryocooler

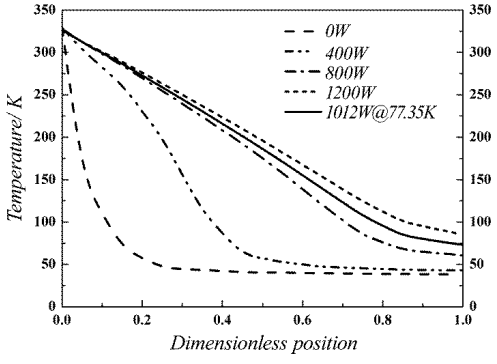

Figure 6. Temperature distribution of working fluid in the regenerator

different cold head heat loads. As shown, the temperature of the working fluid declines nearly linearly along the regenerator under the rated condition (1012 W@ 77.35 K). However, the declining rate is reduced at the cold end of the regenerator. With a lower heat load, a temperature platform forms along a large portion of the regenerator. This temperature platform in the regenerator increases the friction resistance and leads to losses. Figure 6 also shows that a large load benefits from the linearity of temperature profile along the regenerator and the temperature gradient declines. Hence, there is an optimum length for the regenerator in a given working condition.

SUMMARY

A high-power Stirling cryocooler driven by crank-rod mechanisms was simulated numerically using SAGE, showing the phasors of mass flow rate and pressure, the distribution of the enthalpy and the PV power, as well as the temperature distribution along the regenerator under different cold head heat loads. It is shown that the cold head is able to reach the no-load refrigeration temperature of 38 K and a cooling power of 1012 W at 77.35 K with a PV power of 7.72 kW. Based on the analysis of the simulation results, three approaches to optimize the cryocooler have been proposed. The first one is that the phase of the piston and displacer need to be optimized to get an appropriate phase difference (30°, -30°) between flow and pressure oscillations at both ends of the regenerator instead of (-7.1°, -41.6°). The second one is that suitable capacitance and inductance should be added to make the refrigeration system behave as

a resistance to the AC motor. The third one is that the regenerator length should be optimized to a given working condition.

ACKNOWLEDGMENT

This research is financially supported by the National Science Foundation of China (No. 51276156) and State Key Development Program for Basic Research of China (No. 2010CB227303).

REFERENCES

1. Van, D.D., Kes, P., "The discovery of superconductivity," *Physics Today*, Vol. 63 (2010), pp. 38-43.
2. Xu, H.L., Wang, H.L., Wang, J., et al, "Application of cryogenic technology in high temperature superconducting power system," *Cryogenics (Chinese)*, vol. 2 (2003), pp. 20-14.
3. Sun, D.M., Chao, W., Sun, J.C., et al, "Advances in High Power Stirling-Type Pulse Tube Cooler," *Applied Superconductivity, IEEE Transactions on,* Volume: 22, Issue: 3, June 2012 , pp. 2043-2046.
4. Sun, D.M., Dietrich, M., Thummes, G., "Investigation on High-Power Stirling-Type Pulse Tube Coolers for Cooling HTS Motors," *IEEE Transactions on Applied Superconductivity*, Vol. 22, Issue 3, June 2012.
5. Gouge, M.J., Demko, J.A., McConnell, B.W., et al, "Cryogenics Assessment Report," Oak Ridge National Laboratory, Oak Ridge, TN, May 2002.
6. Radebaugh, R., "Cryocoolers: the state of the art and recent developments", *Journal of Physics: Condensed Matter*, Vol. 21, No. 164219 (2009).
7. http://www.stirlingcryogenics.in/home/
8. Bian, S.X., *Miniature cryogenic refrigerators*, China Machine Press, Beijing (1982), pp. 33-45.
9. Gedeon, D., *Sage User's Guide*, Gedeon Associates, Athens, OH. (2011), pp. 97-271.
10. Chen, G.B., Tang, K., *Principles of miniature cryogenic refrigerators*, China Machine Press, Beijing (2009), pp. 97-175.
11. Wu, Y.Z., "Analysis and experimental study of a single-stage pulse tube cryocooler at 120Hz," Zhejiang University, Hangzhou (2011), pp: 93.
12. Chen, T.Q., "Thermodynamic analysis and experimental study of a 3LY-0.8/194 cryocooler," Zhejiang University, Hangzhou (1981), pp: 8-45.
13. Radebaugh, R., "Pulse Tube Cryocooler with Fast Cooldown," 2006.
14. Radebaugh, R., Lewis, M., Luo, E., "Inertance Tube Optimization for Pulse Tube Refrigerators," *Adv. in Cryogenic Engineering*, Vol. 51, Amer. Institute of Physics, Melville, NY (2006), pp. 59-67.
15. Swift, G.W., *Thermoacoustics: a Unifying Perspective for Some Engines and Refrigerators*, Acoustical Society of America, NY (2002), pp. 117.
16. http://en.wikipedia.org/wiki/Power_factor.